Geothermal model at JUNO

Yufei Xi（yufei-xi@qq.com)
Chuanzhi Liao，Guangzheng Jiang (jiangguangzheng@cdut.edu.cn)

Institute of Hydrogeology and Environmental Geology, Chinese Academy of Geological Sciences, Shijiazhuang
School of Energy, Chengdu University of Technology, Chengdu

Neutrino Geoscience, 2026, Zhuhai

Outline

1. Research Background
2. Data
3. Method
4. Results
5. Summary

1. Research Background

■ Geothermal Heat and Geoneutrinos

- Heat flow (Q) is primarily composed of **mantle heat flow (Qm)** and **crustal heat flow (Qc)**. Radiogenic heat production is one of the major sources of crustal heat flow, and the radioactive decay of ^{238}U 、^{232}Th 、^{40}K constitutes the main contribution to heat generation.
- Geoneutrinos are electron antineutrinos produced by the natural beta decay of radioactive elements in Earth's interior.

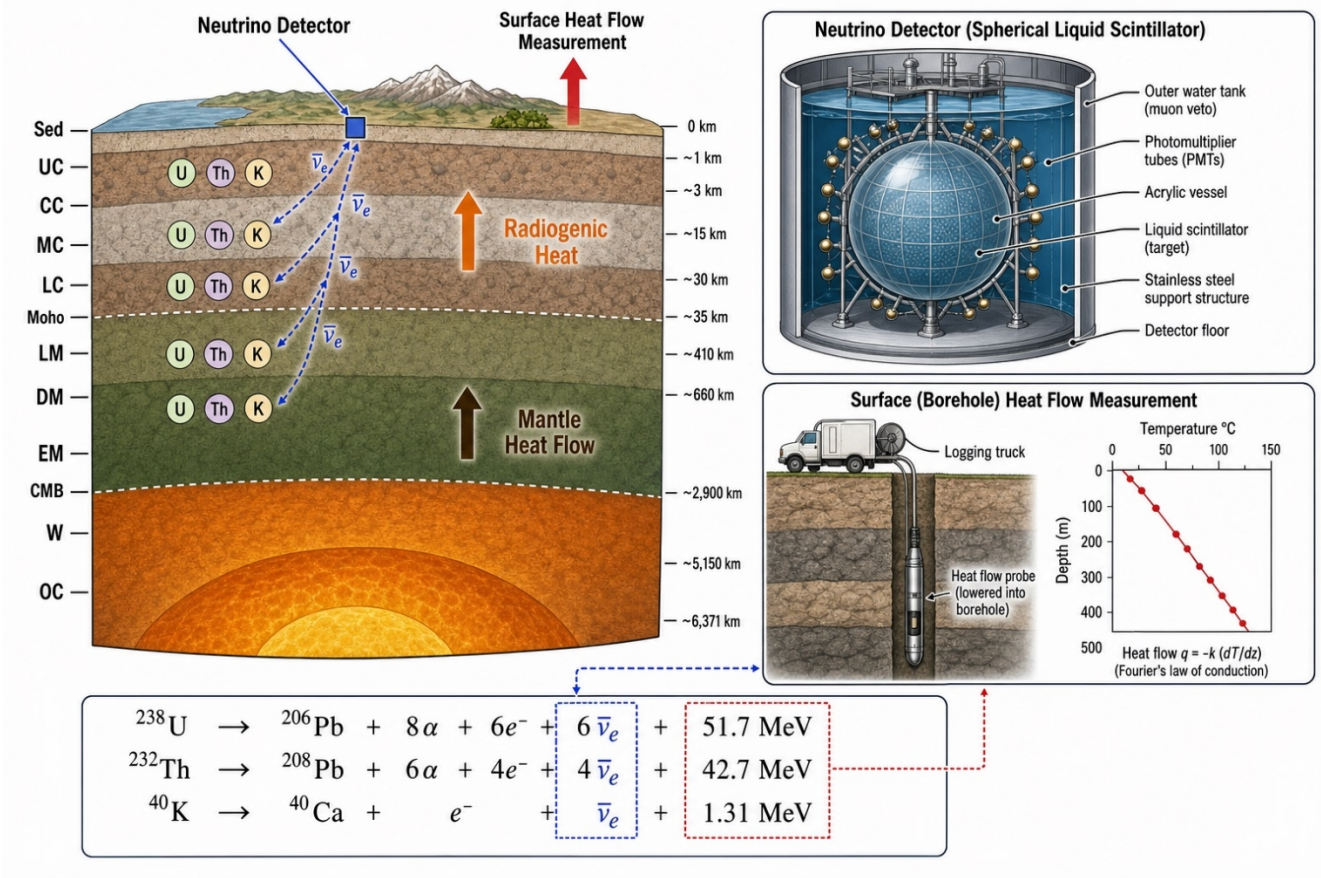

heat production(mW/m³) $A = 0.01\rho(9.52C_U + 2.56C_{Th} + 3.48C_K)$

During the decay of ^{238}U 、^{232}Th、^{40}K, geoneutrinos and radiogenic energy are released in a fixed proportion.

1. Research Background

■ Terrestrial Heat Flow in China

- Thermal state of continental China: **higher in the southwest and east, low in the northwest and the central region**. (**2337** terrestrial heat flow measurements).
- In eastern China, the average heat flow in the northern part is 65 mW/m², while the average heat flow along the **southeastern coast reaches 75 mW/m²**. (surface heat flow differs by 15%)

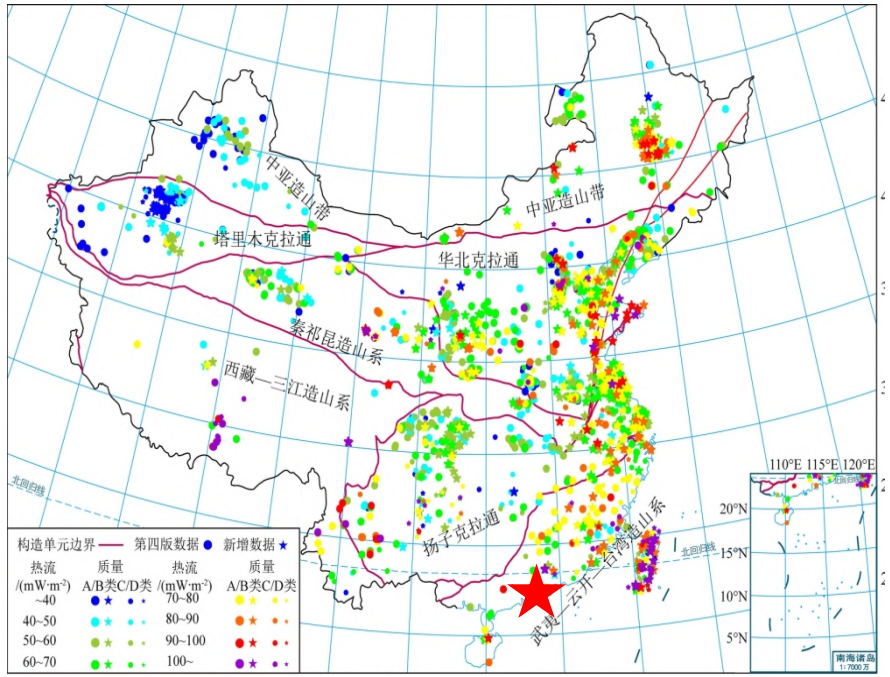

Distribution of heat flow measurements in China (5th edition) (Wang et al., 2025)

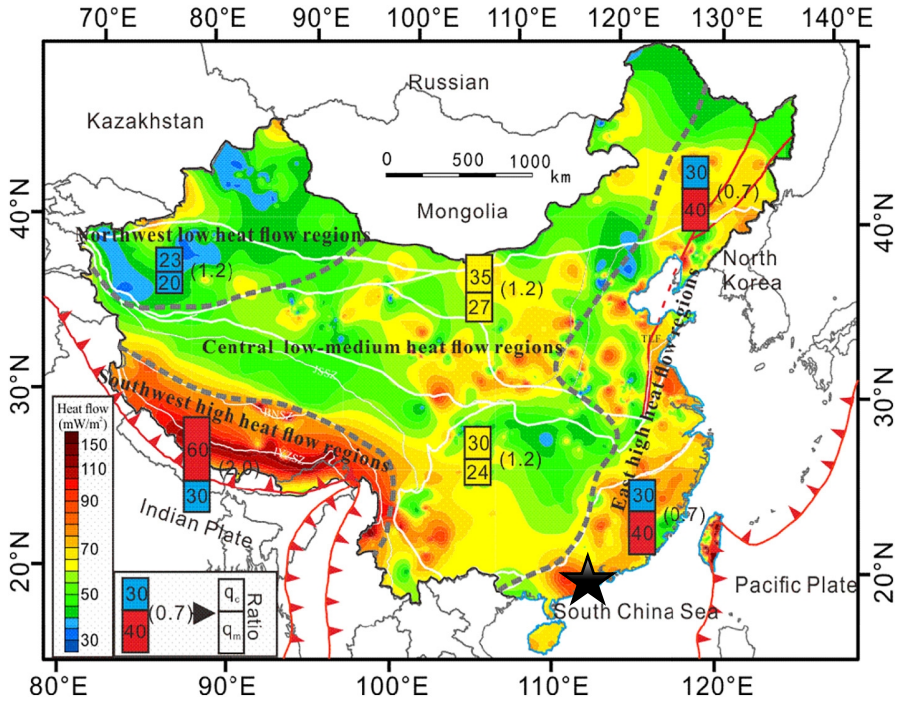

Terrestrial heat flow distribution and heat-source mechanism zoning in China (Jiang et al., 2019)

1. Research Background

Granite intrusions in Southestern China

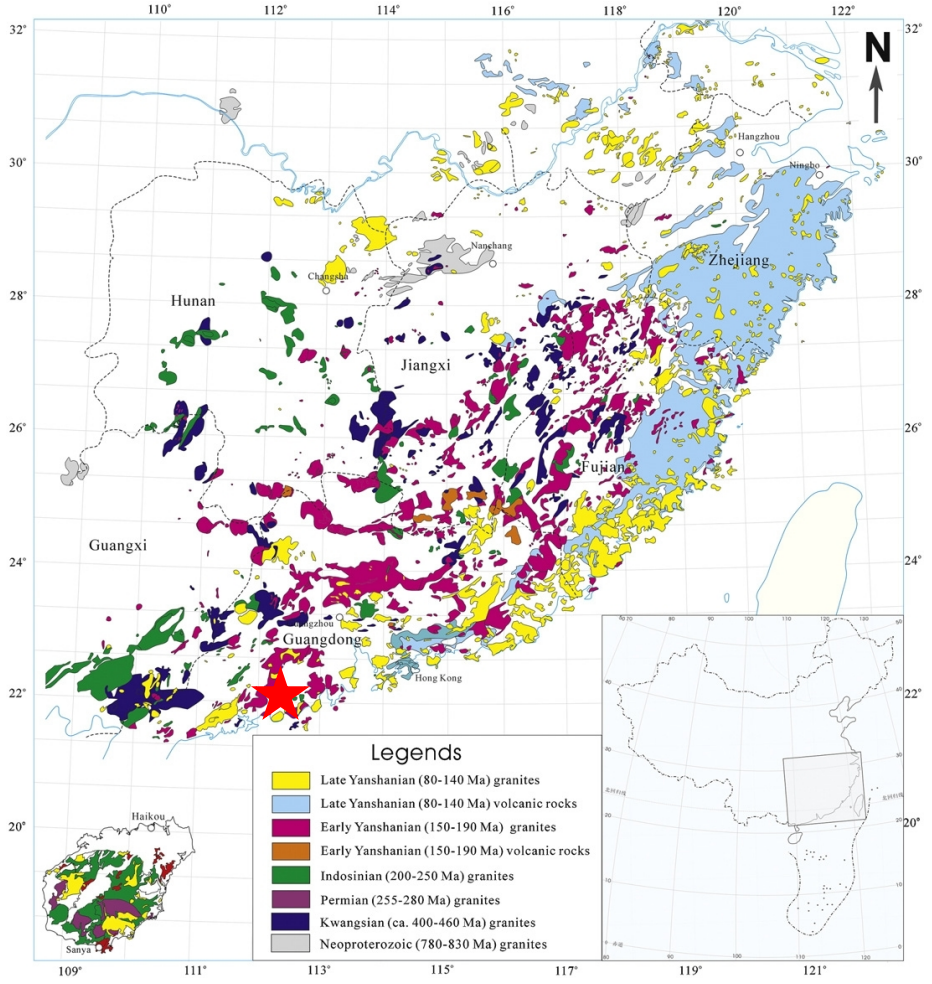

Granites in the eastern South China Block(Wang et al.,2013)

Southeasten China has experinced multi-stage magmatic intrusions, with high heat production (As) and high heat flow (Qs).

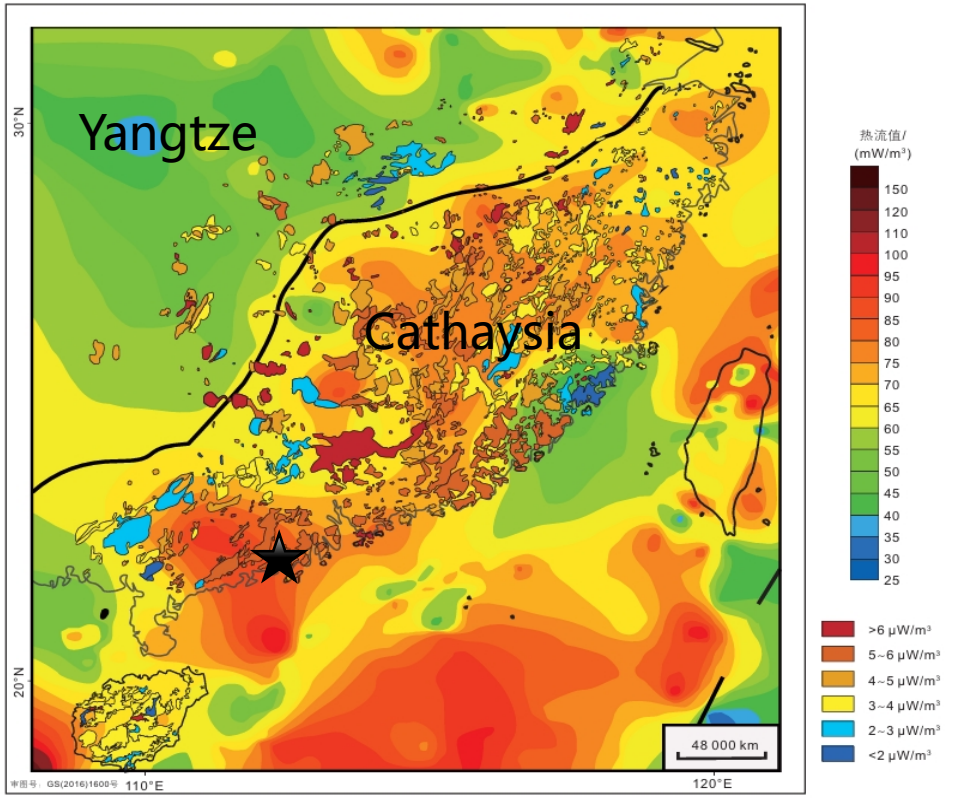

Granite heat production and heat flow in South China(Li et al., 2023)

1. Research Background

■ Heat flow–heat production relation (Q–A)

The empirical Q–A relation

$$Q_s = Q_r + D^*A_s$$

Q_s: surface heat flow √

A_s: surface heat production √

Q_r: reduced heat flow

D: effective depth scale

(Roy et al., 1968; Lachenbruch, 1970)

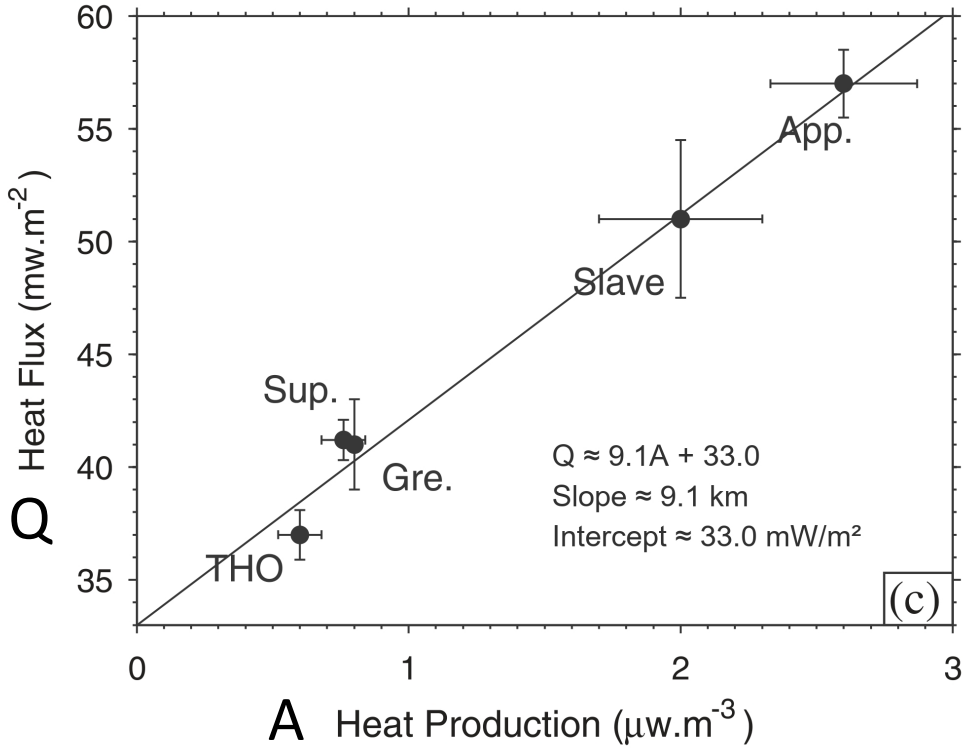

Q-A relation(Jaupart, et al., 2016)

1. Research Background

■ Vertical models and the radiogenic enrichment layer

Classical vertical profiles

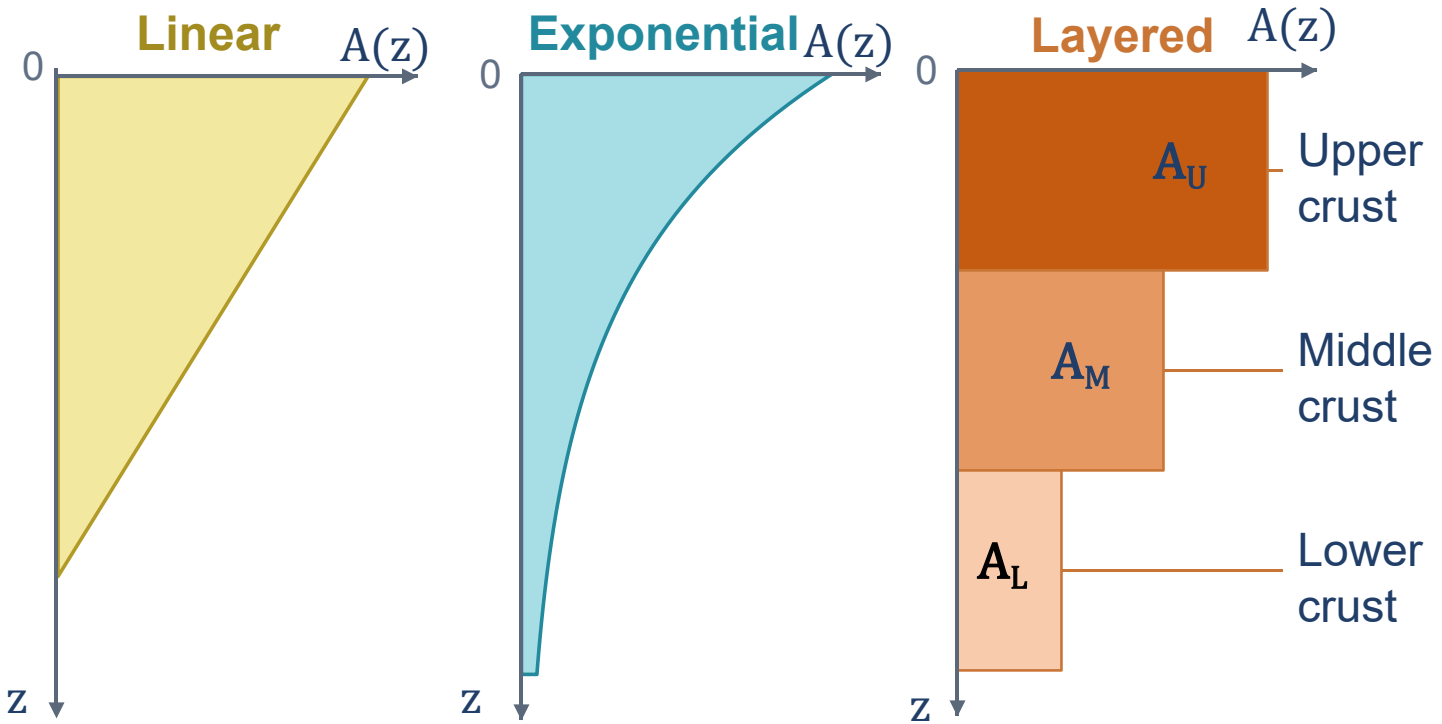

$A(z) = A_0 - \beta z$ $A(z) = A_0 \exp(-z/D)$ A_U, A_M, A_L

Three Decreasing Models for the Distribution of A with depth(Lachenbruch, 1970)

Geothermal model at JUNO

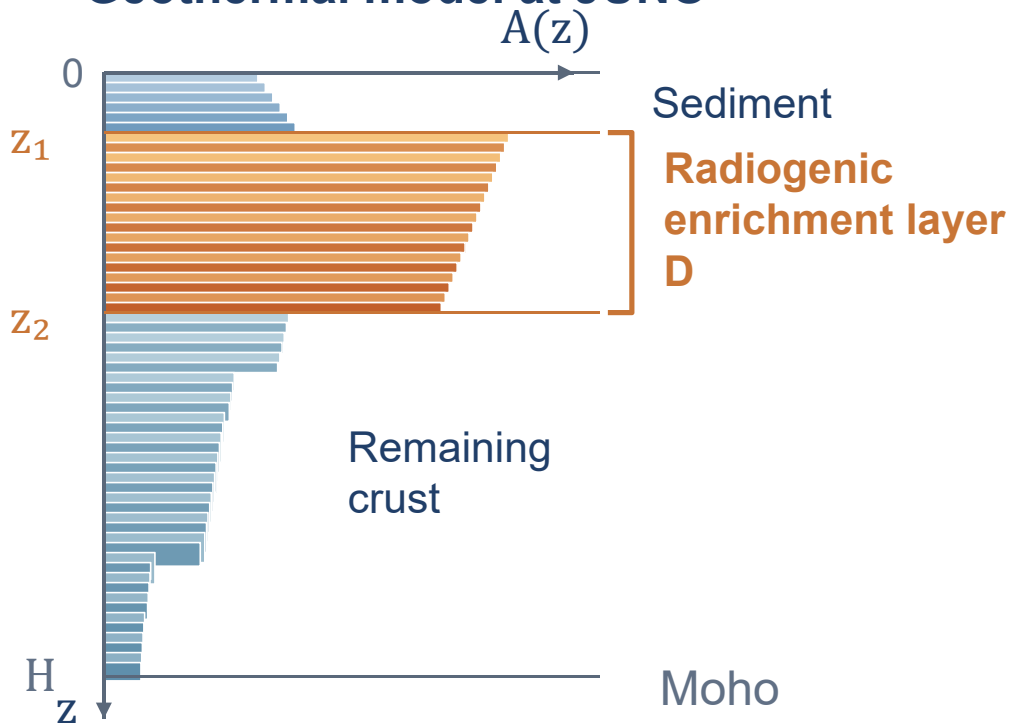

Radiogenic enrichment layer

An upper-crustal interval with higher U–Th–K abundances than the deeper crust(Jaupart et. al, 2016).

Heat flow constrains the integrated heat production. Deep constraints help locate the enriched interval.

1. Research Background

■ Why deep constraints are needed

Surface samples do not resolve deep sources.

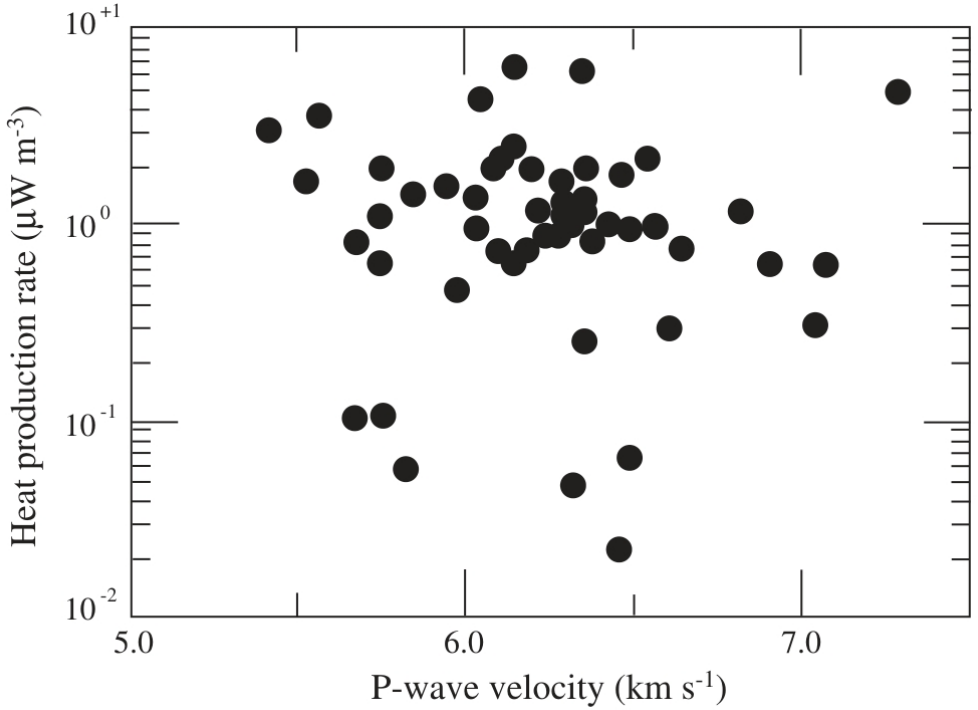

Similar Vp, widely varying heat production(Jaupart et al., 2016)

Empirical Vp–A relation(Rybach & Buntebarth, 1984)

$$\ln A = 12.6 - 2.17\, V_p$$

A: $\mu W/m^3$ V_p: km/s (at 100 MPa)

■ Our approach for South China

01 Seismic structure + rock data

Infer lithology probabilities at depth and assign U–Th–K distributions.

02 Crustal heat-flow balance

Separate mantle heat flow and constrain D under the chosen vertical model.

03 A 3-D source model for JUNO

Predict the U–Th geoneutrino signal with uncertainty in composition and depth.

2. Data

Heat flow measurement :Long-term Temperature Monitoring at JUNO

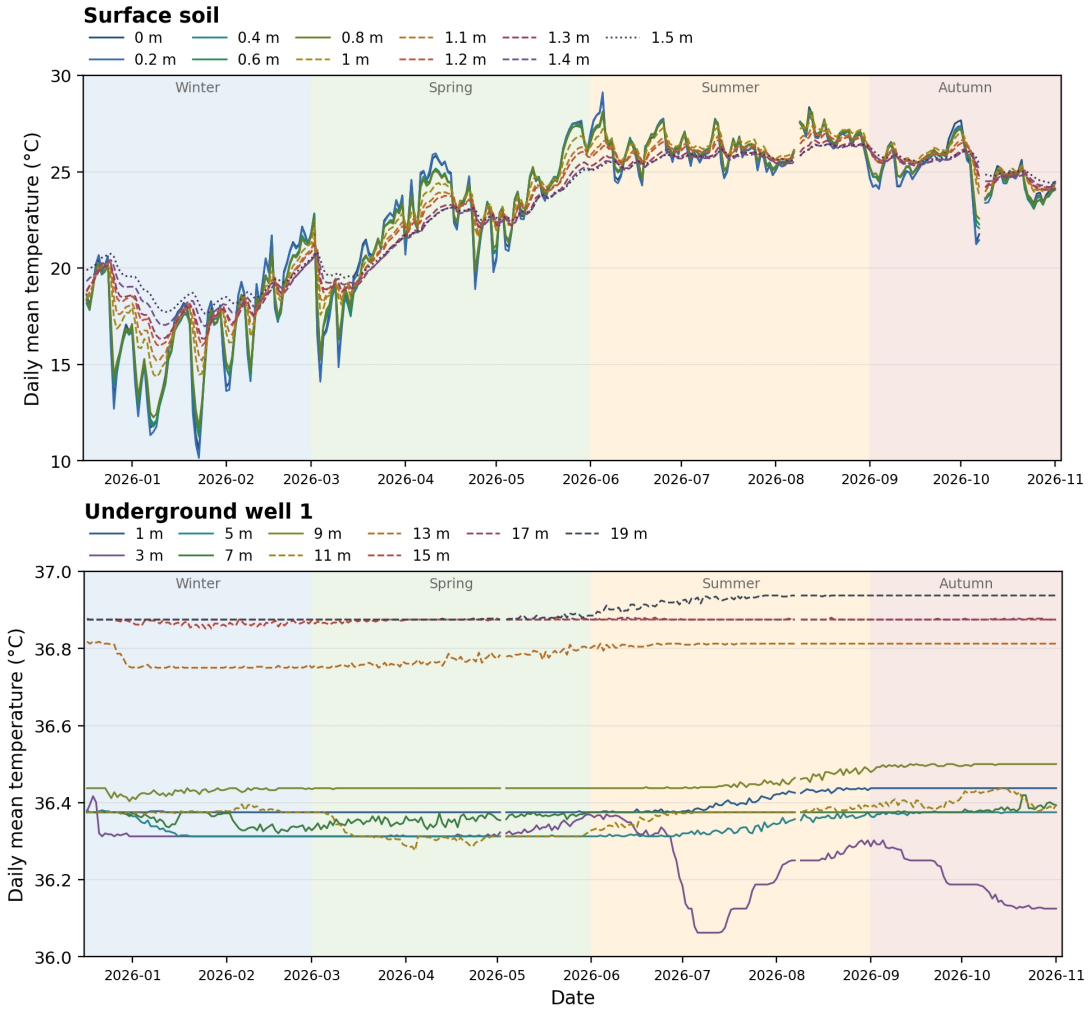









Long-period temperature observations at JUNO

2. Data

New Heat-flow mesurements in South China

Well	Longitude (°E)	Latitude (°N)	Depth (m)	Gradient (°C/km)	Conductivity (W/m/K)	Heat flow (mW/m²)
FSR1	110.187	20.014	4900	32.4	2.57	83.3
X6	110.049	20.342	3500	28.2	2.50	70.5
X8	110.024	20.321	3500	26.3	2.52	66.3
JUNO	112.512	22.120	700	24.8	3.23	80.10







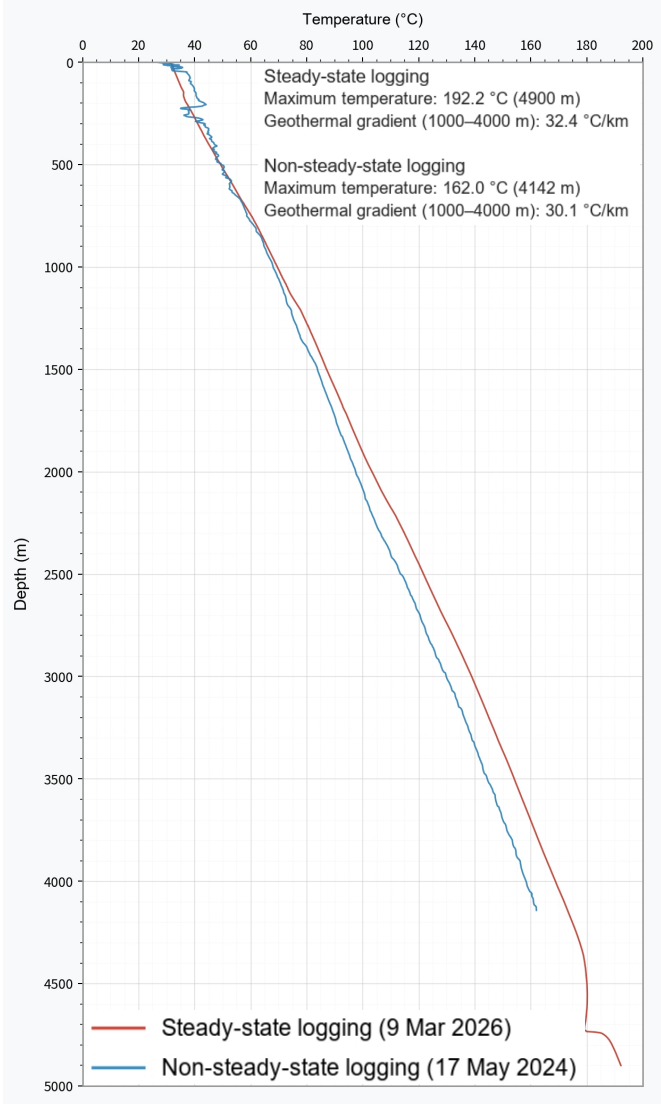

temperature profile of Haikou FSR1 well

2. Data

■ Heat-flow patterns in South China

➢ We compiled 521 recently published heat flow data points for South China and **added 4 new heat flow measurements**, yielding an average value of **75.3 mW/m²**.

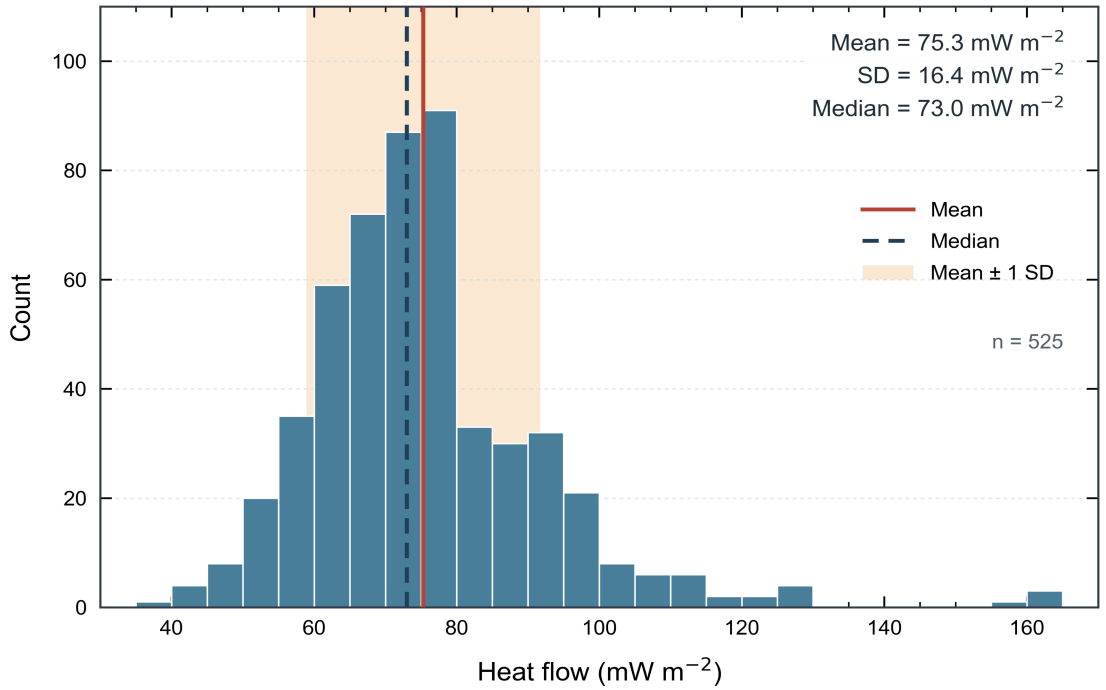

Heat flow histogram for South China

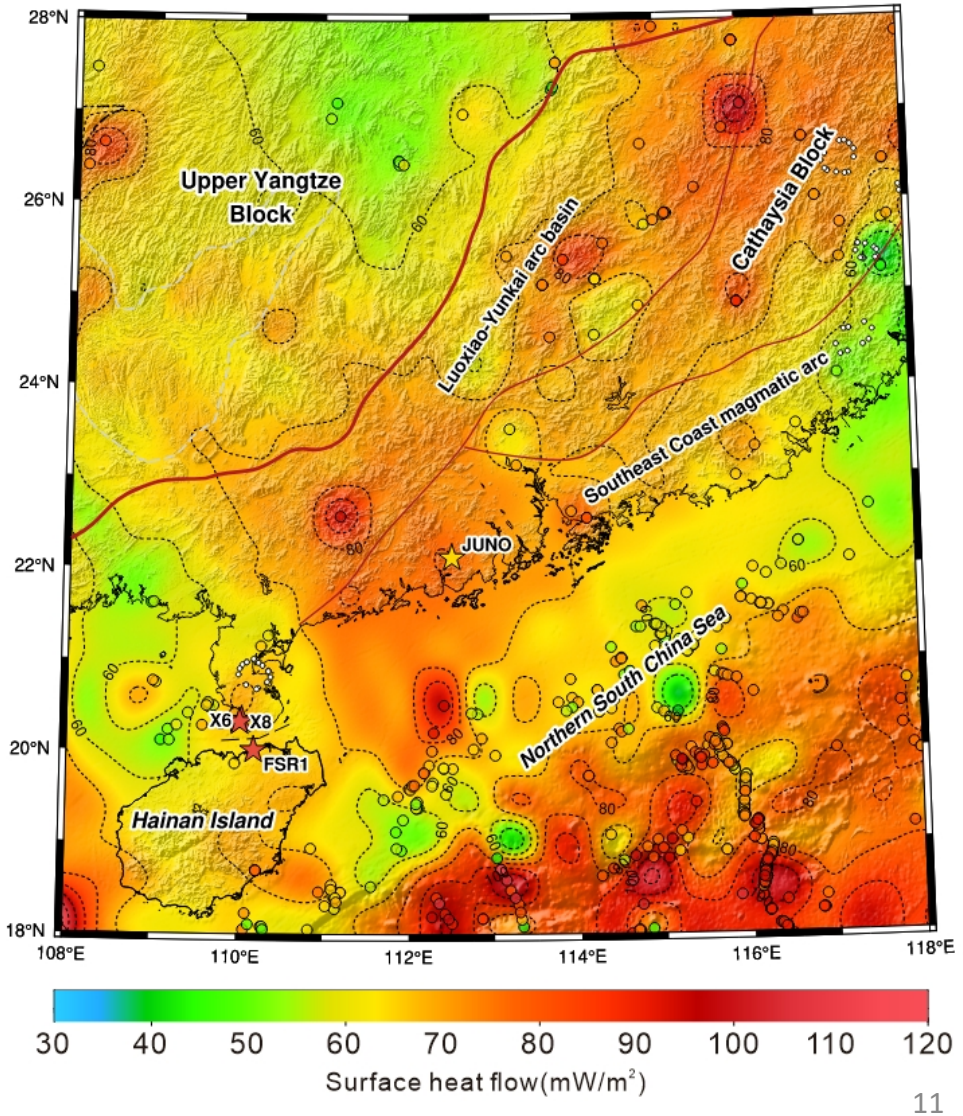

Distribution of Heat Flow in South China

2. Data

Heat-flow patterns in South China

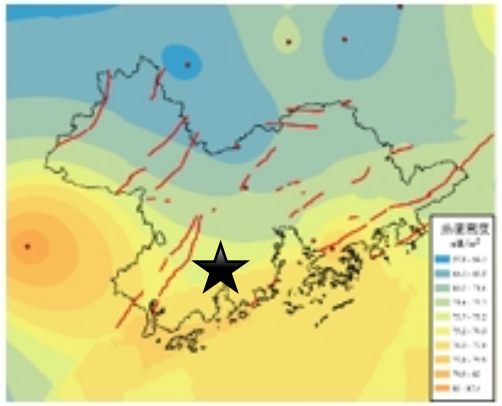

Heat flow map, before

~75mW/m^2

Prof. Huang’ s talk, from fall school

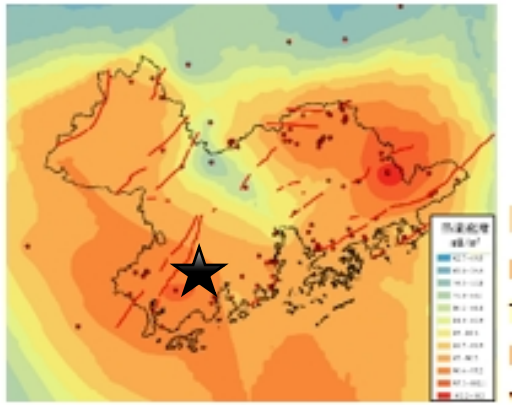

Heat flow map, after

>80 mW/m^2

Heat flow around JUNO could be even higher.

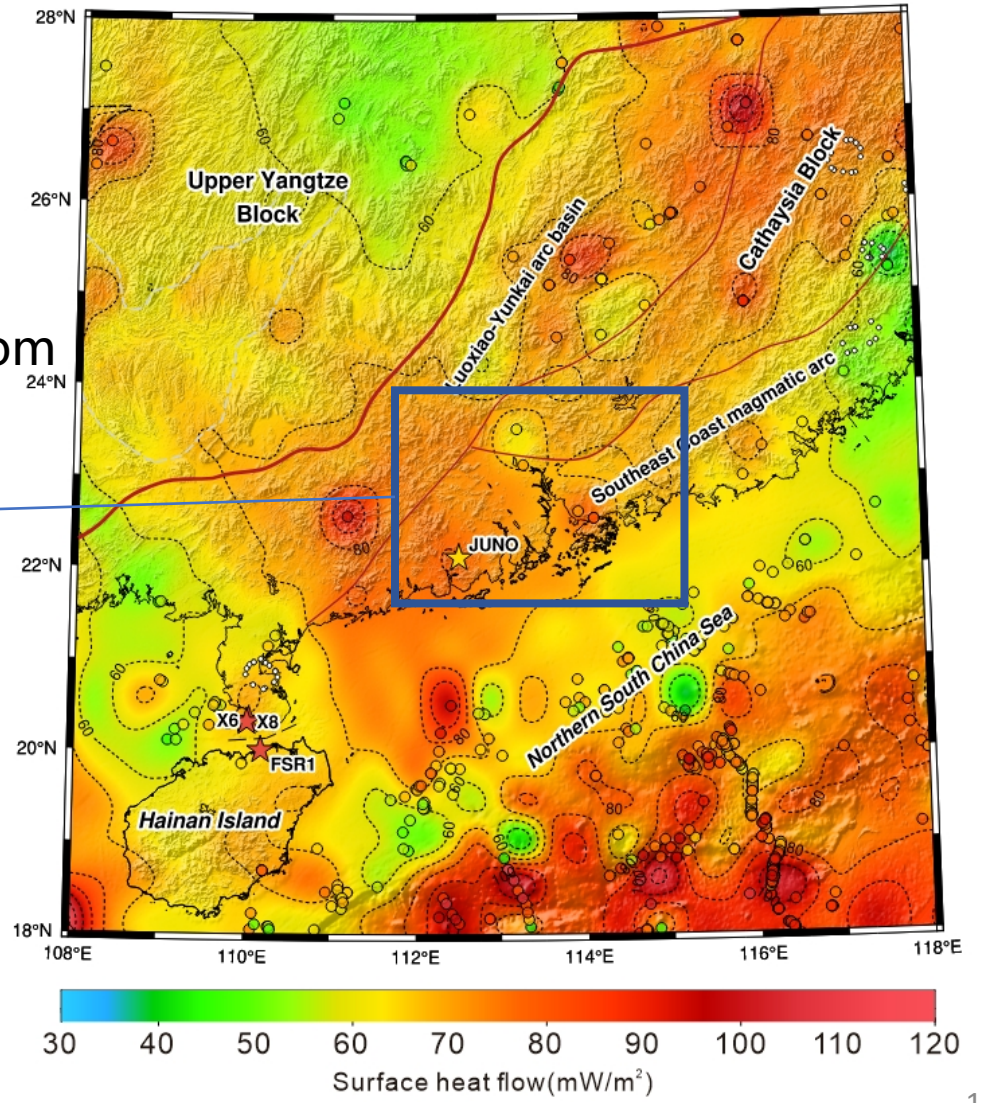

Distribution of Heat Flow in South China

2. Data

Radiogenic heat production patterns in South China

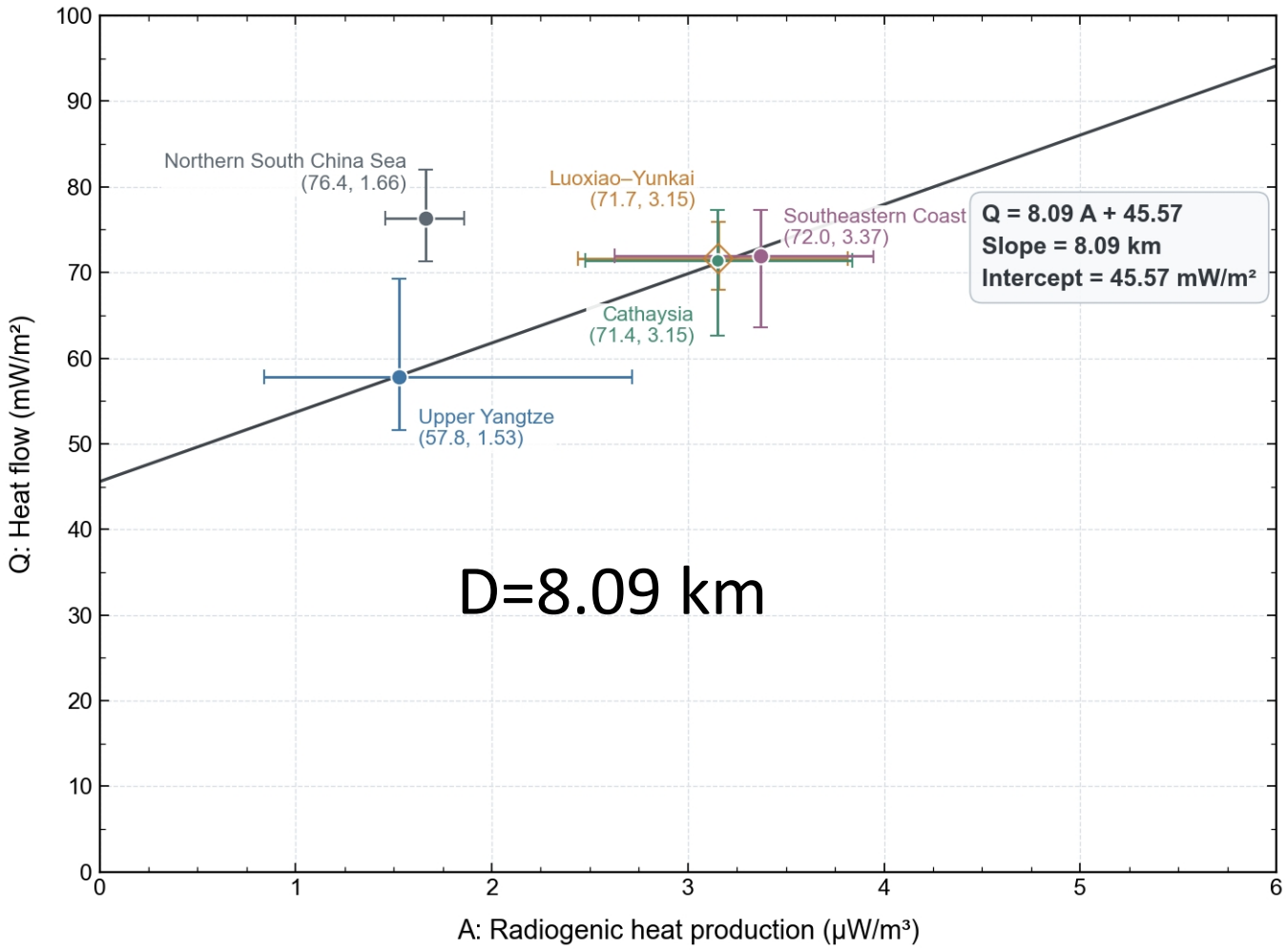

Q-A relation in South China

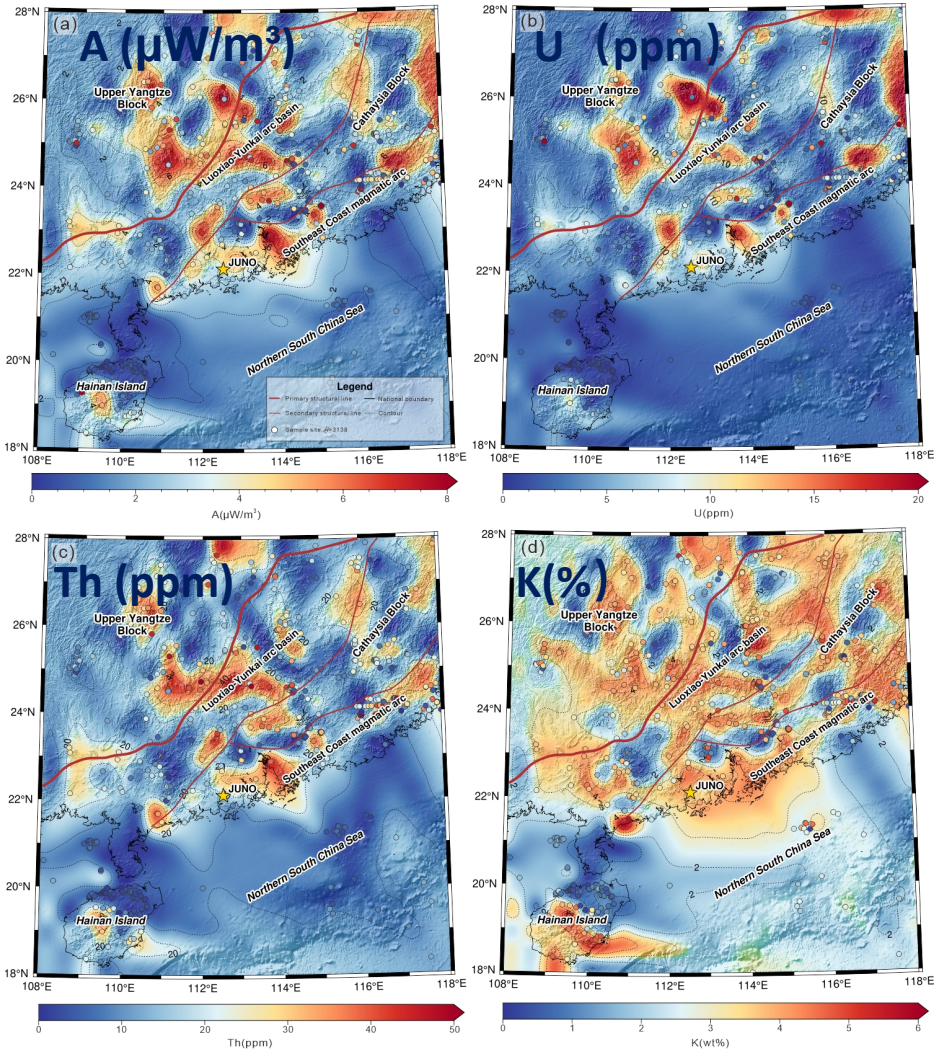

Sample heat production and U–Th–K abundances.

2. Data

Radiogenic heat production patterns in South China

- This study compiled crustal rocks across South China(Sun et al., 2022; Li, et al., 2023). The lithological data are presented in the figures.

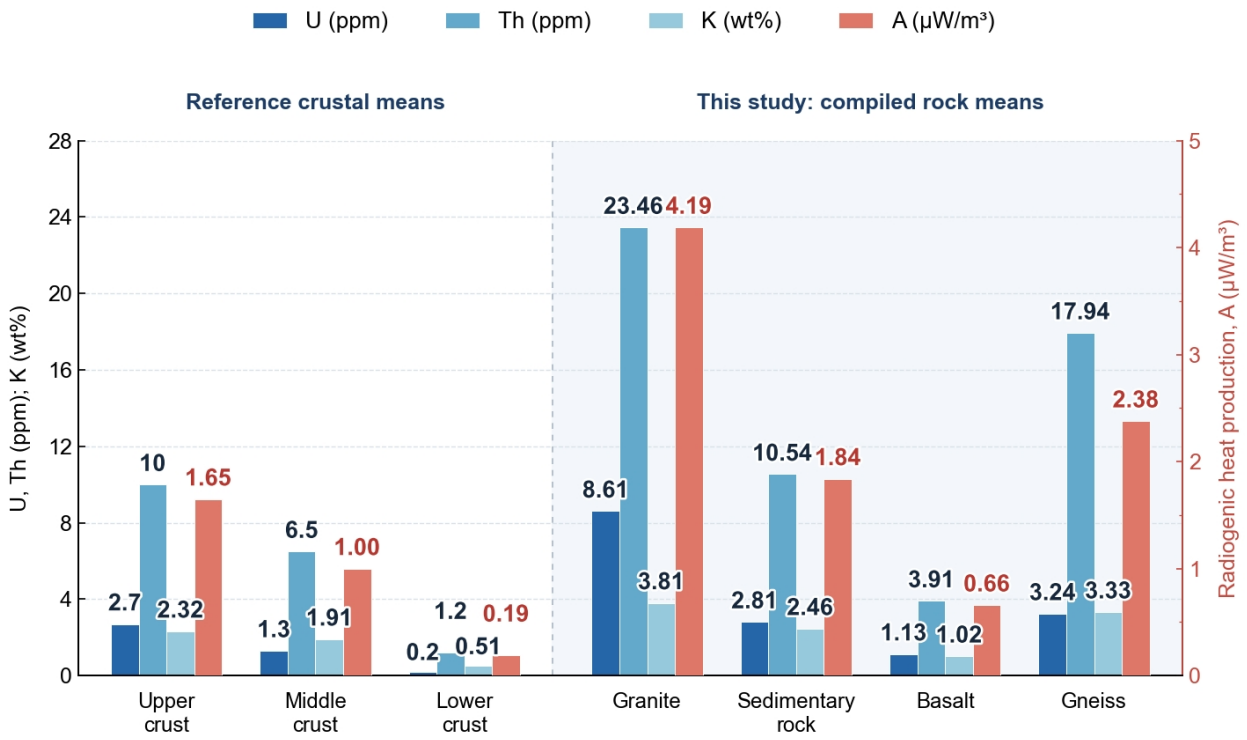

Average U, Th, and K_2O Abundances and Radiogenic Heat Production in the Continental Crust(Rudnick & Gao, 2003; Taylor & McLennan, 1985)

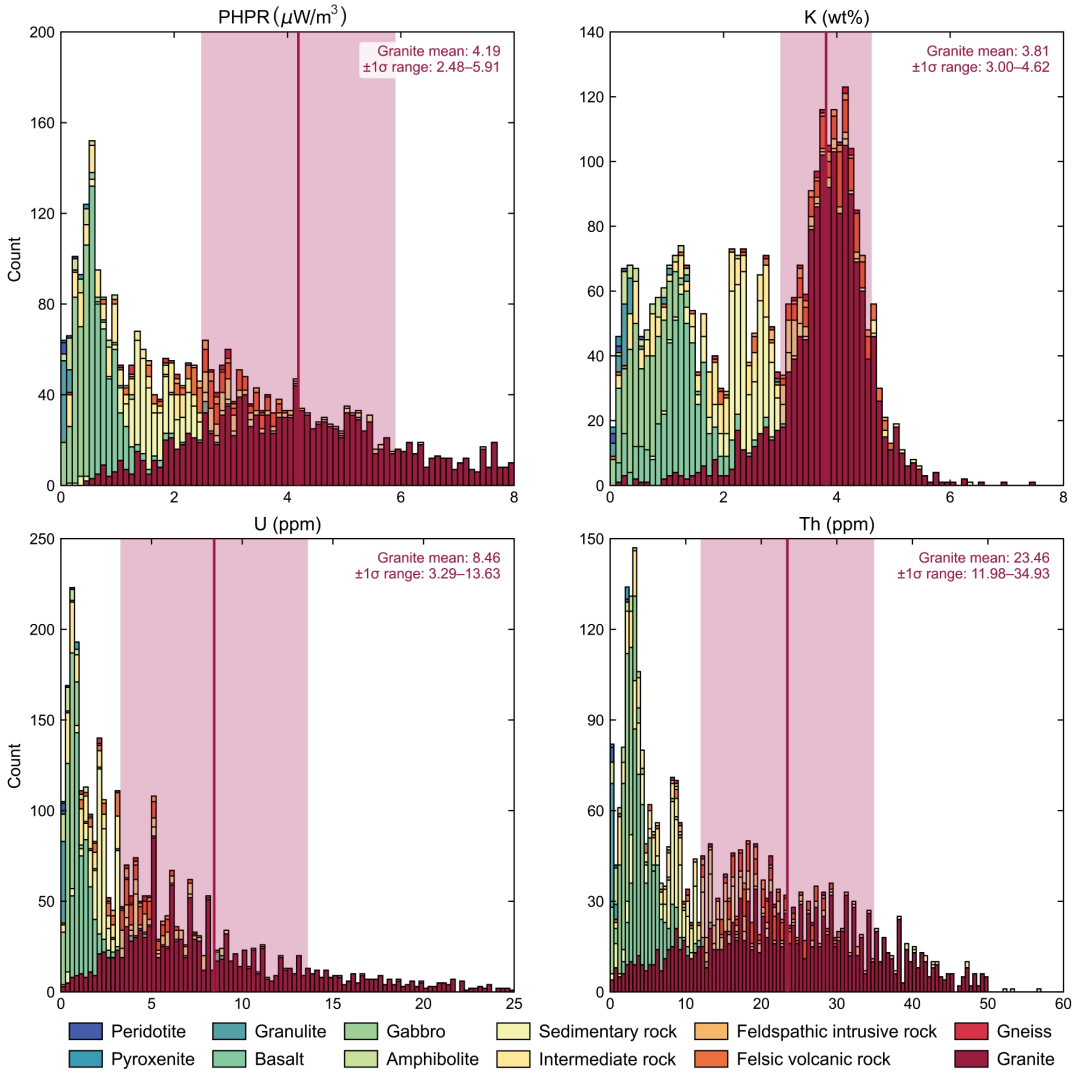

Histogram of Radiogenic Heat Production Rate and U-Th-K Abundances in South China

3. Method

Differences from the JULOC-I Method

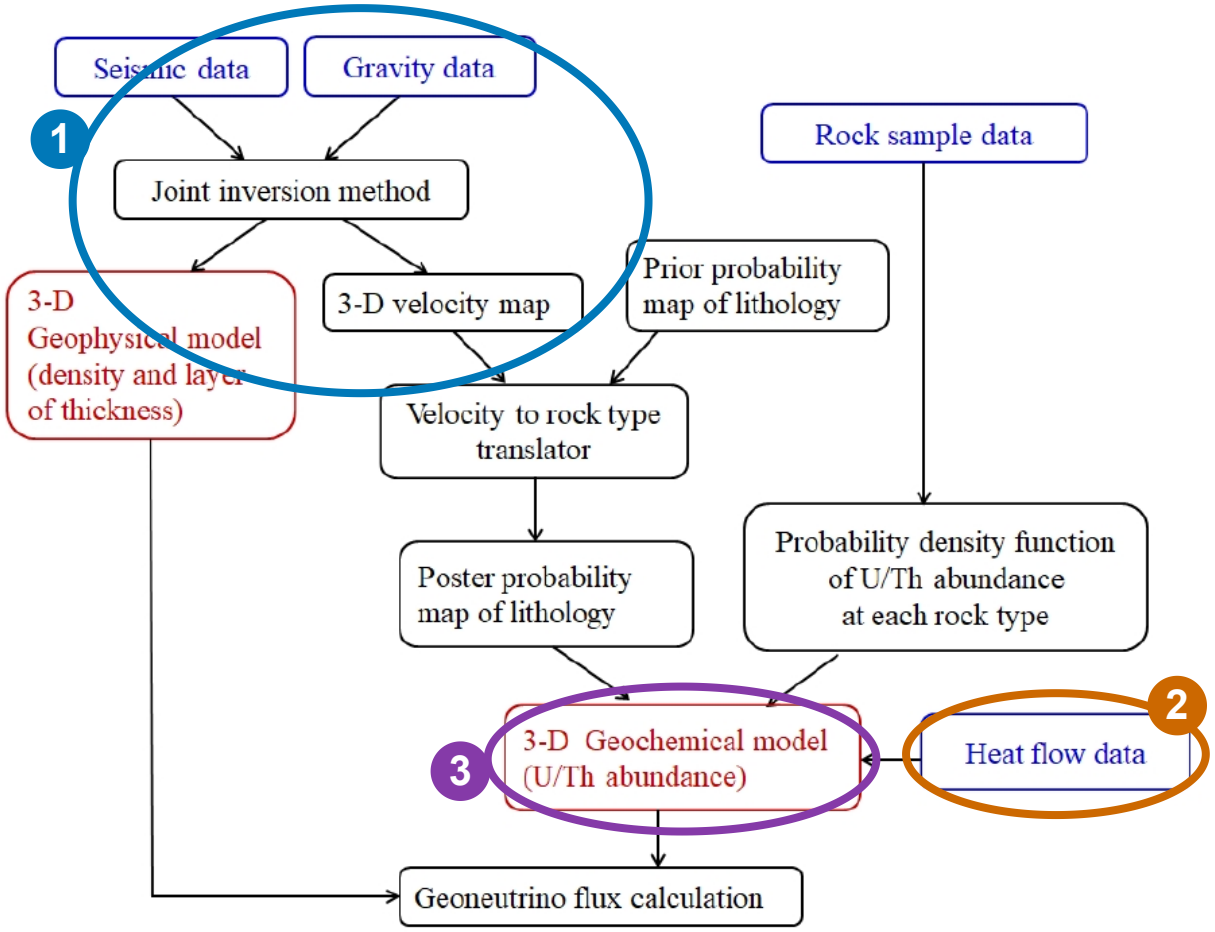

JULOC-I workflow

1 Seismic model and velocity inputs

JULOC-I: joint inversion of seismic and gravity data.

This study: CSRM-1.0 Vp for crustal lithology, Vs for mantle temperature and mantle heat flow.

2 Role of the heat-flow constraint

JULOC-I: Qc is from crustal composition
Qm = Qs − Qc checks the model.

This study: Qm is from mantle Vs.
Qc = Qs − Qm, Qc constrains crustal composition.

3 Enrichment thickness D

JULOC-I: 3-D U–Th model in seismic crustal layers.

This study: scan D and update lithological priors. Recompute A–U–Th–K and match Qc.

$$Q_{c,model}(D) = \int A(z; D)\, dz \approx Q_c$$

3. Method

Differences from the JULOC-I Method

$$q_s = q_c + q_m$$

surface

Crustal contribution

Moho flux

$$q_c = \sum_1^n (A_i \cdot D_i)$$

A_iD_i: heat production and thickness of each layer

	JULOC-I model	Geothermal model
Study area	108°E-118°E, 18°N-28°N	108°E-118°E, 18°N-28°N
Grid size	0.4°*0.4°*1km	0.4°*0.4°*0.5km
Geophysical structure	Local Gravity + Seismic model	CSRM1.0 model
Rock samples	Sun et al.,2022	Sun et al.,2022;Li et al.,2023
Thermal Constraint	Qm>=15mW/m^2	Qm from Seismic prediction

3. Method

■ Step 1: Separation of crustal and mantle heat flow in South China

CSRM1.0 Model (Xiao et al, 2024)
0.4°×0.4°×0.5km
Moho–120 km
Vs data

→

V2RhoT_gibbs (Kumar, 2020 and 2022)
Vs → Mantle Temperature

→

Linear fitting
Moho–120 km
Mantle geothermal gradient

→

Qm
Gradient × thermal conductivity=
mantle heat flow

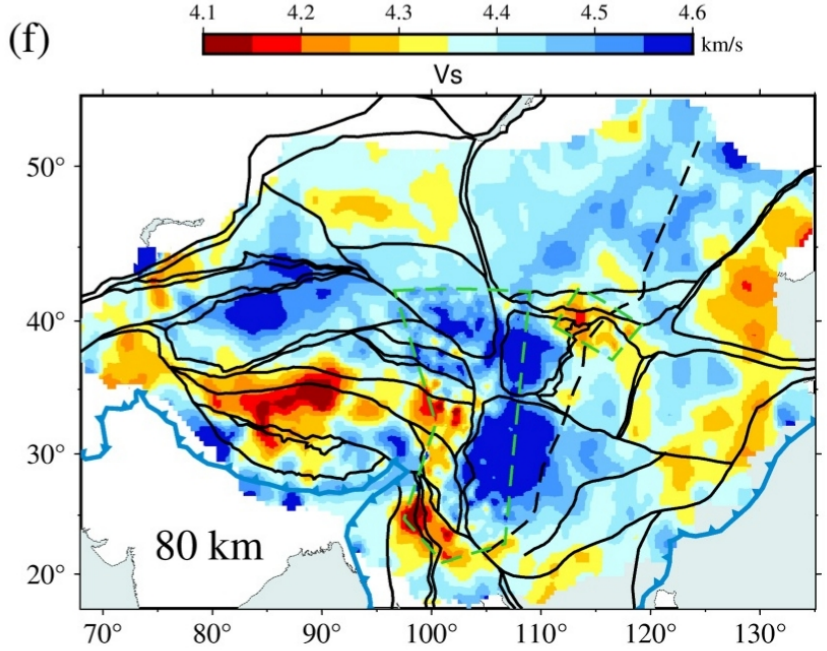

CSRM-1.0: Vs at 80 km(Xiao, et al.,2024)

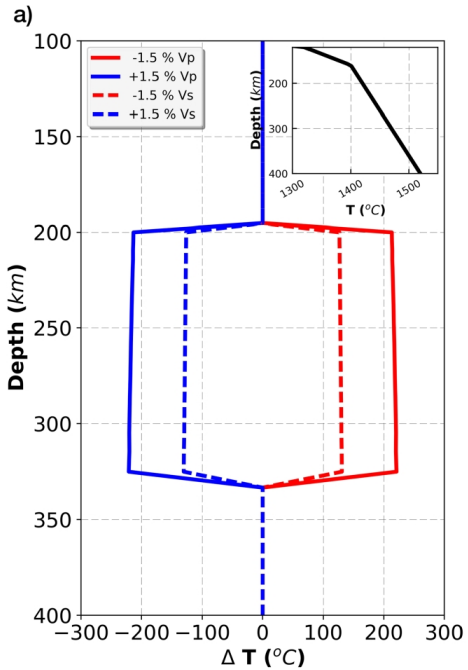

Vp and Vs: thermal sensitivity(Kumar et al., 2020)

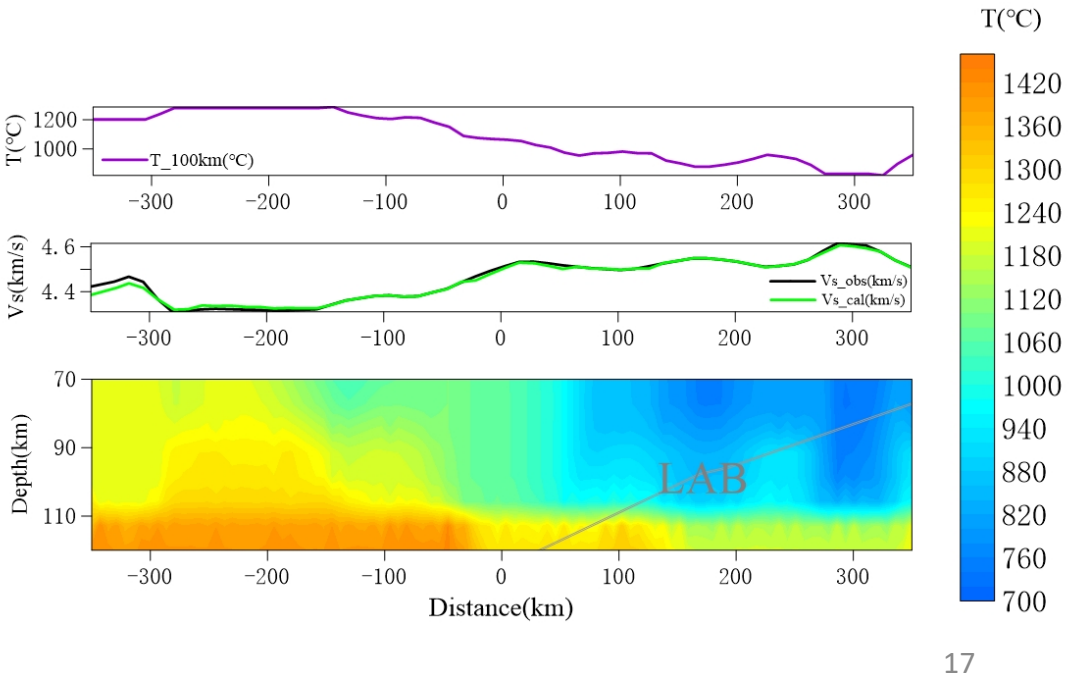

2-D Temperature Cross-Section

3. Method

- **Step 1: Separation of crustal and mantle heat flow in South China**

Surface Heat Flow (Qs) − **Mantle Heat Flow (Qm)** = **Crustal Heat Flow (Qc)**

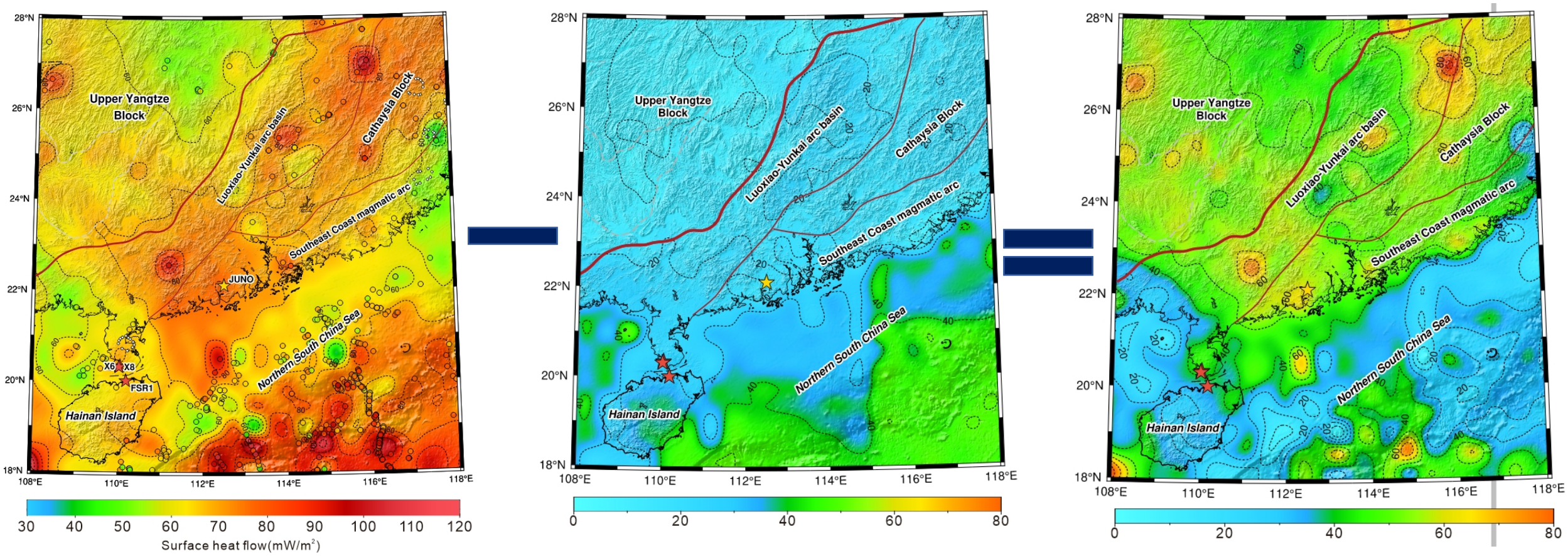

Key constraints on radiogenic enrichment layer thickness

3. Method

Step 2: Independent crustal heat-flow constraints determine enrichment thickness

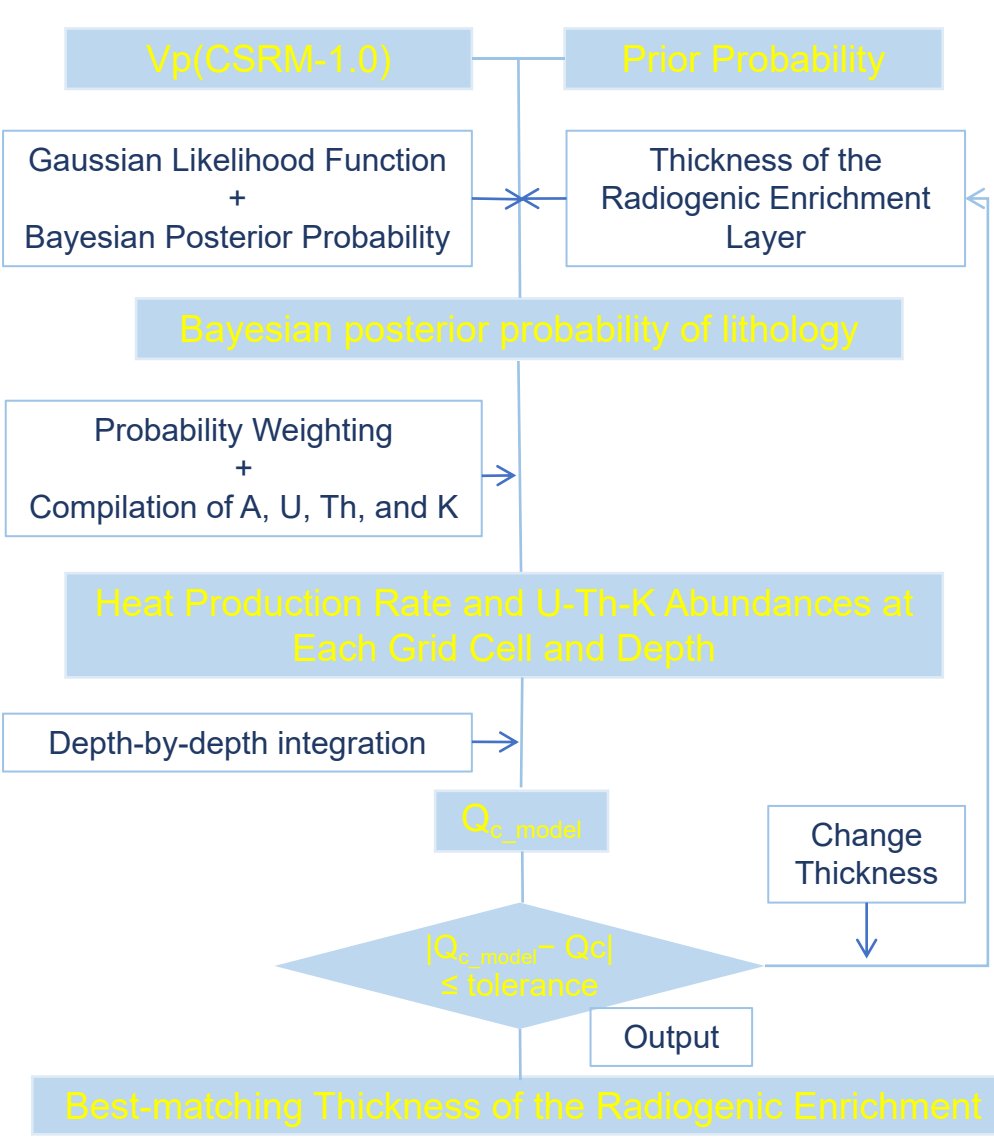

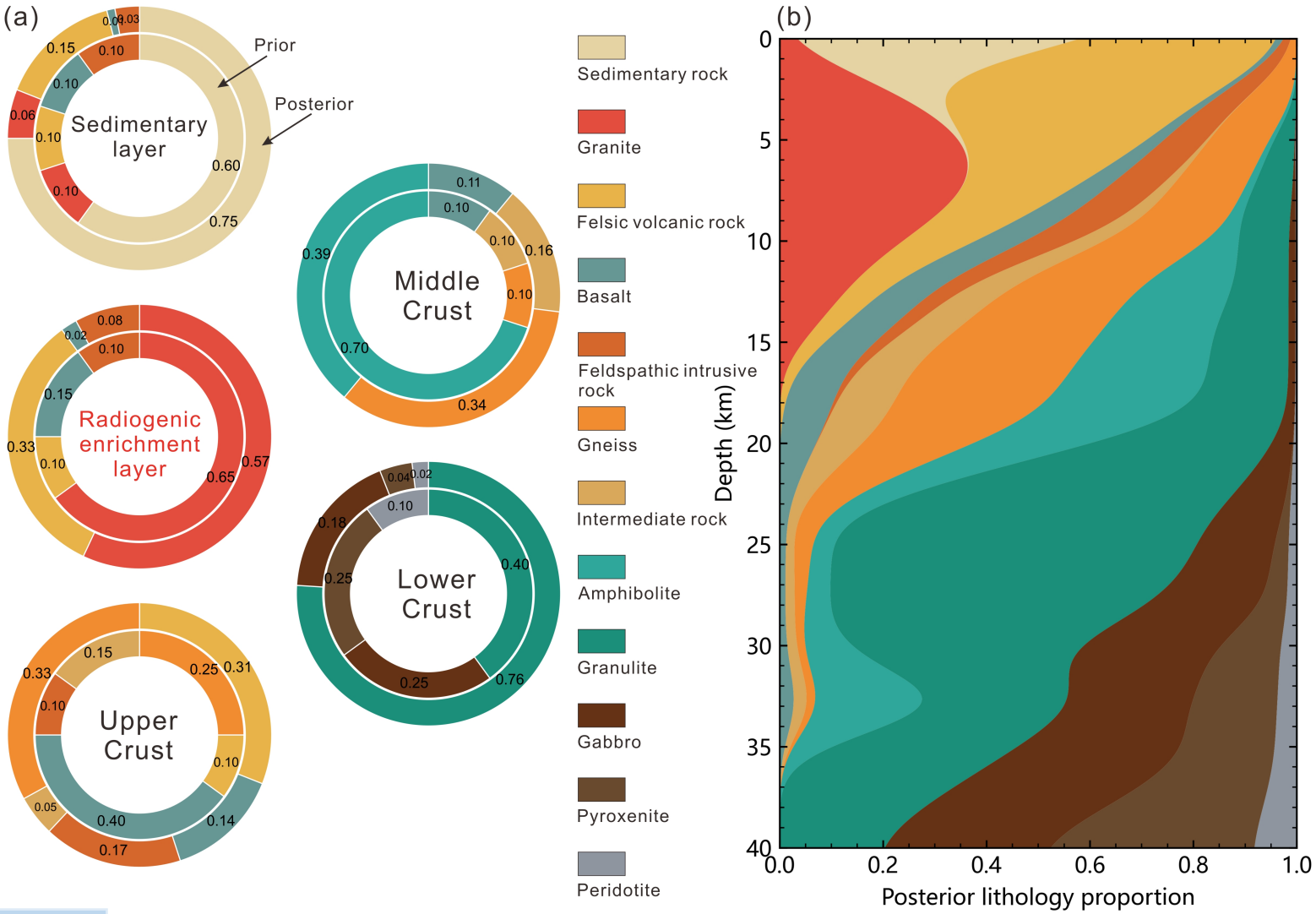

4. Results

Radiogenic enrichment layer(D) in South China

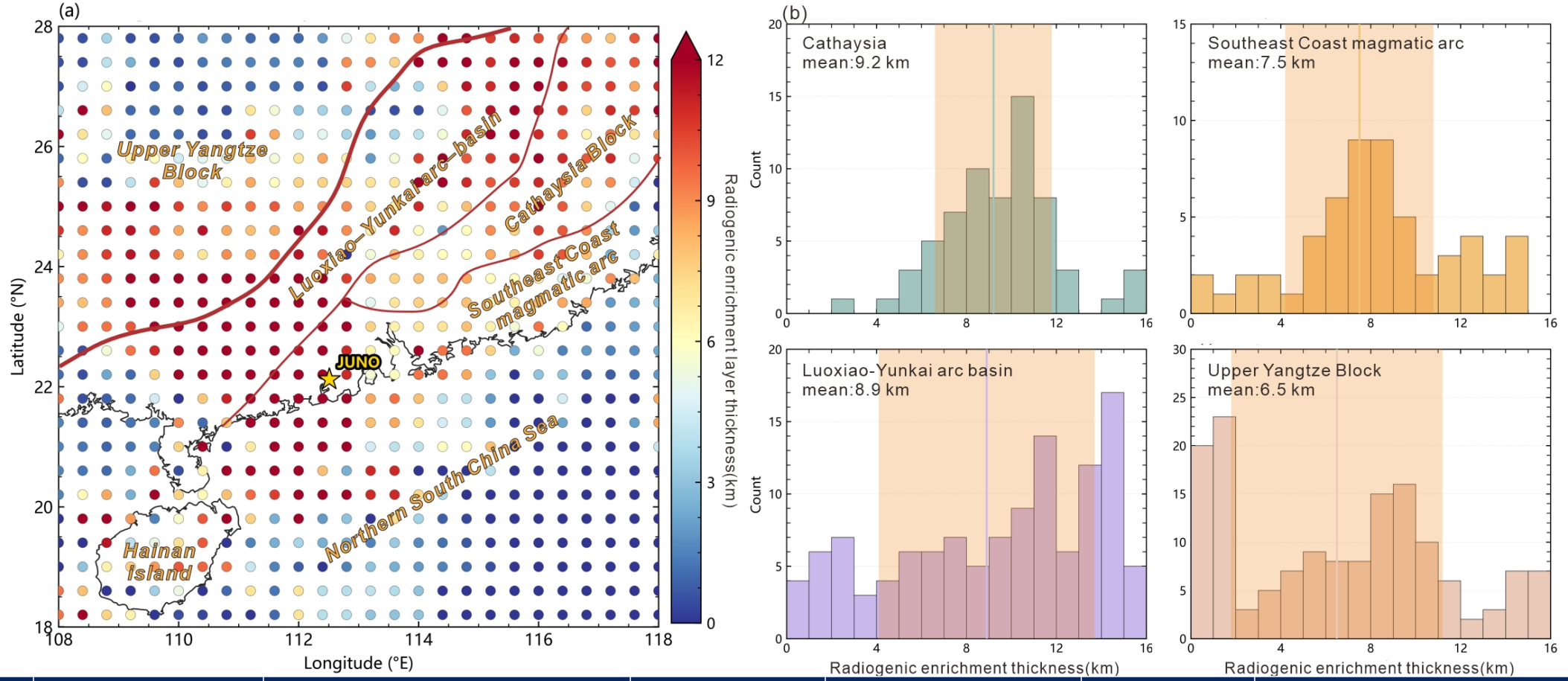

Tectonic unit	Upper Yangtze Block	Luoxiao–Yunkai arc–basin system	Cathaysia Block	Southeastern Coastal Magmatic Arc	Hainan Island	Northern South China Sea	Overall
D (km)	6.5	8.9	9.2	7.5	5.9	4.7	6.9

4. Results

■ Radiogenic enrichment layer(D) in South China

- ➢ High A is concentrated in the shallow crust. The thickness and heat production of the radiogenic enrichment layer shows significant lateral variations.

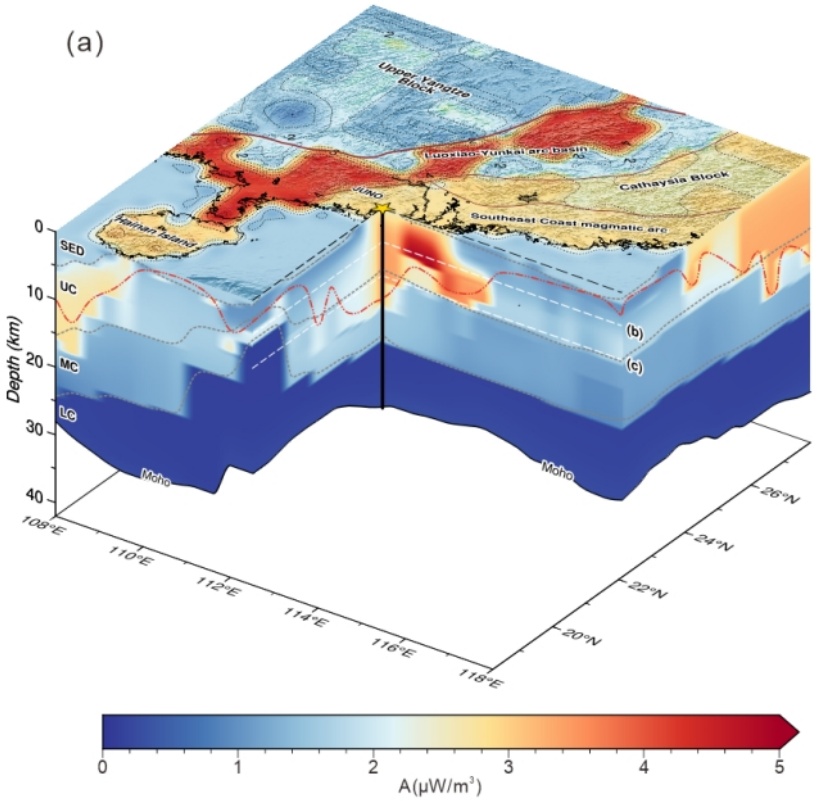

Three-dimensional cutaway of A centred on JUNO

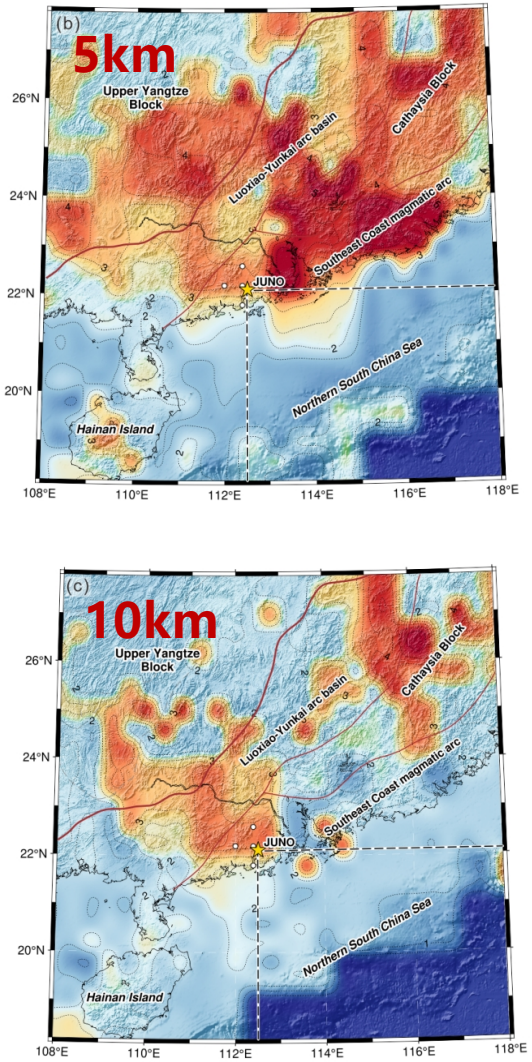

Posterior A at 5 km and 10 km

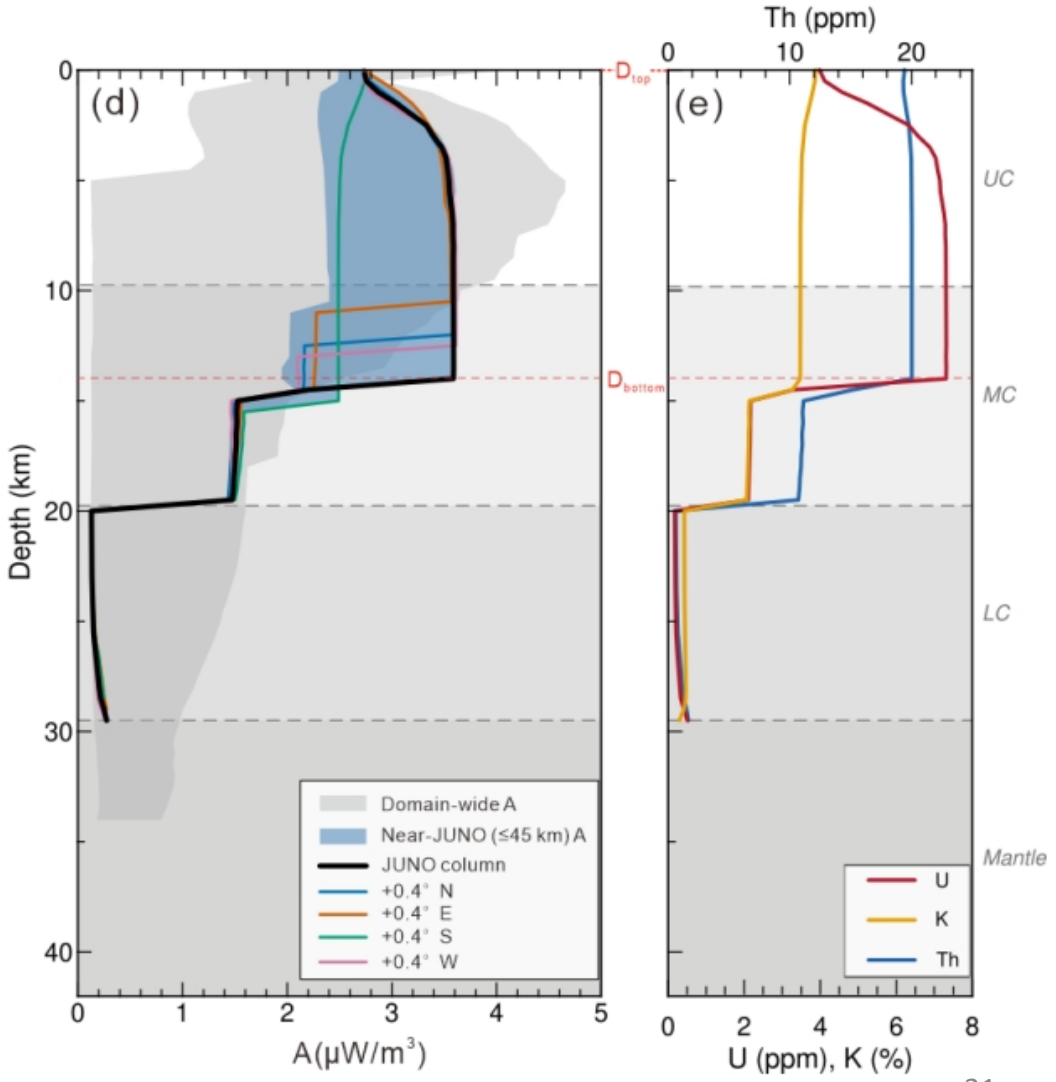

Vertical A profiles and Posterior U, Th and K for the JUNO grid column

4. Results

Geoneutrino signal prediction at JUNO

Predicted geoneutrino signals at JUNO(TNU)

Component	S_U	S_{Th}	S_{TOT}
LOC	$27.8^{+2.5}_{-5.0}$	$6.8^{+0.3}_{-0.4}$	$34.6^{+2.5}_{-5.0}$
FFC	$7.6^{+1.6}_{-1.6}$	$2.3^{+0.2}_{-0.2}$	$9.8^{+1.7}_{-1.7}$
Bulk crust	$35.4^{+3.0}_{-5.3}$	$9.1^{+0.4}_{-0.5}$	$44.4^{+3.0}_{-5.3}$
CLM	$1.3^{+2.4}_{-0.9}$	$0.4^{+1.0}_{-0.3}$	$2.1^{+3.0}_{-1.3}$
Lithosphere	$36.7^{+3.8}_{-5.4}$	$9.5^{+1.1}_{-0.6}$	$46.5^{+4.0}_{-5.4}$
DM	4.2	0.8	4.9
EM	2.9	0.9	3.8
Total	$43.8^{+3.8}_{-5.4}$	$11.2^{+1.9}_{-0.8}$	$55.3^{+4.0}_{-5.4}$

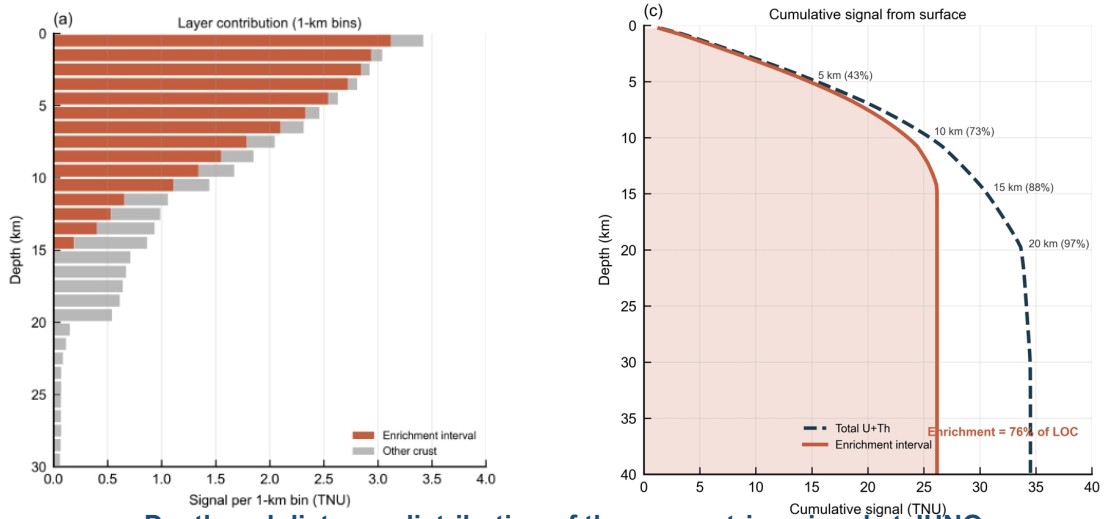

Depth and distance distribution of the geoneutrino signal at JUNO

Lithospheric geoneutrino signals comparison at JUNO

Modle	LOC Area	S(U+Th)[THU]		
		LOC	ROC	CLM
RMM	6°×4°	$16.4^{+3.0}_{-2.6}$	$11.7^{+2.3}_{-1.9}$	$2.1^{+2.9}_{-1.3}$
GIGJ	6°×4°	$14.4^{+2.5}_{-2.4}$	$11.7^{+2.2}_{-1.9}$	$2.1^{+2.9}_{-1.3}$
W20[Crust_2.0]	6°×4°	$16.9^{+4.3}_{-3.4}$	$11.8^{+3.3}_{-2.6}$	$1.7^{+2.9}_{-1.1}$
W20[Crust_1.0]	6°×4°	$16.7^{+4.4}_{-3.5}$	$11.7^{+3.3}_{-2.6}$	$1.7^{+2.9}_{-1.1}$
W20[Lithos_1.0]	6°×4°	$17.1^{+4.5}_{-3.6}$	$12.7^{+3.6}_{-2.8}$	$0.6^{+0.9}_{-0.4}$
JULOC	10°×10°	$28.5^{+4.5}_{-4.5}$	$9.8^{+1.7}_{-1.7}$	$2.1^{+2.9}_{-1.3}$
Geothermal	10°×10°	$34.6^{+2.8}_{-5.3}$	$9.8^{+1.7}_{-1.7}$	$2.1^{+2.9}_{-1.3}$

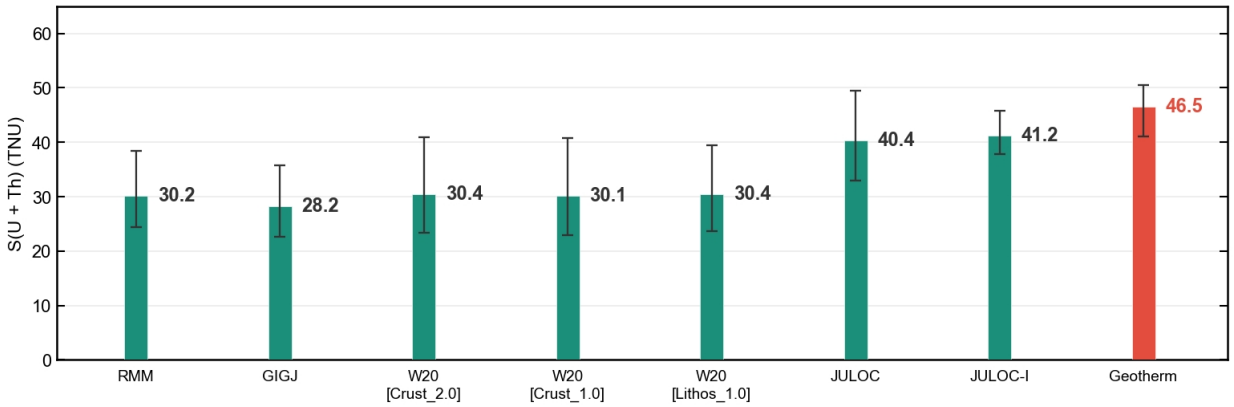

Comparison of predicted geoneutrino signals at JUNO.

5. Summary

- Based on the JULOC-I model, we established a geothermal model using more sampling data, updated seismic models, and additional heat flow data constraints.
- The overall heat flow enrichment layer(D) is 6.9 km thick in the South China Block from the geotherm model, compared to 8.09 km from the simple Q-A diagram.
- Our 3-D model predict the highest geoneutrino flux for the lithosphere (**46.5 +4.0/−5.4 TNU**).
- Future work might indicates that, higher surface heat flow around JUNO (Shaopeng Huang‘s talk) and higher upper crustal abundances (Kang Chen’s talk) may lead to a higher geoneutrino flux prediction for JUNO.